

Understanding Heating of the Solar Corona Through Soft X-ray Spectroscopy

A. Caspi¹, A. Y. Shih², H. P. Warren³, A. R. Winebarger⁴, M. C. M. Cheung⁵, C. E. DeForest¹, S. Gburek⁶, J. A. Klimchuk², M. Kowaliński⁶, G. T. Laurent¹, J. P. Mason⁷, T. Mrozek⁶, S. E. Palo⁸, M. Schattenburg⁹, R. A. Schwartz², D. B. Seaton^{1,10}, M. Stęslicki⁶, J. Sylwester⁶, & T. N. Woods⁷

¹SwRI; ²NASA GSFC; ³NRL; ⁴NASA MSFC; ⁵LMSAL; ⁶CBK PAN; ⁷CU/LASP; ⁸CU/AES; ⁹MITLL; ¹⁰CU/CIRES

Why is the solar corona orders of magnitude hotter than the underlying chromosphere and photosphere? After more than 80 years^[1,2], this “coronal heating problem” remains one of the fundamental unanswered questions in solar physics^[3]. Magnetohydrodynamic simulations and observations of convective flows^[4] suggest that the Sun’s complex magnetic field is an efficient conduit for energy transport from the solar interior and subsequent storage in the corona, but the mechanism for releasing that energy to heat the corona to millions of Kelvin remains unknown.

Decades of astrophysical observations have established that soft X-ray (SXR; $\sim 0.1\text{--}10$ keV) emission provides unique diagnostics, not available from other wavelengths, of such high-energy processes in stellar coronae. Despite the rich insights enabled by spectrally resolved SXR measurements, similar observations of the Sun have been sporadic (Fig. 1), with incomplete coverage of the crucial $0.25\text{--}3$ keV ($4\text{--}50$ Å) range and with significant compromises between spectral, spatial, and temporal resolution. Emerging advances in detectors, focusing optics, diffraction gratings, and other technology offer both near- and long-term capabilities to completely fill this observational gap with imaging spectroscopy at high resolution, sensitivity, and cadence. **Significant progress into the critical coronal heating question – and other closely related questions – is easily achievable by 2050 if we leverage these advances and prioritize development of new solar SXR observatories^[5,6].**

Models based on impulsive dissipation of magnetic complexity through reconnection (“nanoflares”^[7]) suggest that coronal plasma should be routinely heated to flare-like, $\sim 5\text{--}10$ MK temperatures, but with relatively low density^[8,9]. In contrast, models based on wave dissipation predict narrower, cooler coronal temperature distributions^[10,11]. Observations showing hot emission from the active Sun^[12–14] and much cooler emission from the quiet Sun^[15] appear to support low-frequency nanoflare heating for active regions but a different mechanism – such as small-scale flux cancellation^[16] – for the quiet network. However, the difficulty of measuring weak, high-temperature emission – particularly using extreme ultraviolet (EUV) observations – has led to inconsistent results and multiple, conflicting interpretations^[17–20].

Solar flares produce copious high-temperature plasma at temperatures up to $\sim 30\text{--}50$ MK^[21,22]. Flare emission is easily observable but the mechanism that drives this heating nonetheless remains poorly understood. It is commonly accepted that much of the flare thermal plasma results from chromospheric material “evaporating” into the corona as it is heated by collisions from non-thermal, downward-accelerated electrons^[23,24]. However, numerical simulations of this process^[25,26] have difficulty reproducing the “super-hot,” >30 MK plasma observed in intense flares. A growing body of evidence^[21,22,27–31] suggests that a significant fraction of the thermal plasma – especially

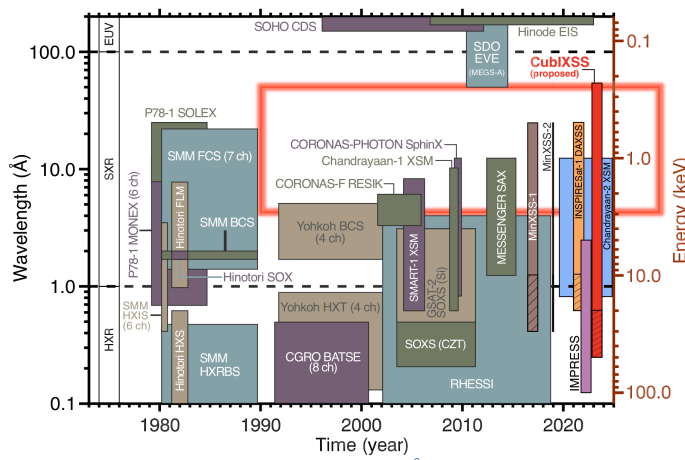


Fig. 1. The crucial $0.25\text{--}3$ keV ($4\text{--}50$ Å) range, highlighted, has never been fully covered by spectrally resolved observations, and has been studied only sporadically in recent years.

in the hot tail of the temperature distribution – is heated *in situ*, directly in the corona. This hottest plasma, particularly the super-hot component, exhibits fast dynamics during the impulsive phase and can precede the onset of hard X-ray (HXR) emission from flare-accelerated electrons^[21,23], suggesting its sensitivity to the details of the energy release process^[22,29]. However, the exact mechanism for *in situ* heating, and its relationship to non-thermal particles, remains strenuously debated^[24,26,32]. Particle-associated heating may even be driven by non-thermal ions instead of electrons, but more detailed measurements of ions are needed^[33].

Measurements of elemental abundances in hot coronal plasma provide crucial information on how mass flows within, and into, the corona in response to heating. It is well established that the composition of the solar atmosphere varies from photosphere to corona^[34], with variations organized by first-ionization potential (FIP) whereby low-FIP abundances tend to be enhanced in the corona relative to the photosphere (the “FIP bias”).

Abundance measurements thus test models of hot plasma origin, but studies so far have yielded mixed results, complicated by aforementioned observational difficulties (including possible non-equilibrium ionization) and likely by different temperature sensitivities of the lines studied. Some recent SXR observations suggest a near-photospheric composition for high-temperature quiescent active region plasma^[14], while prior EUV studies have generally shown coronal FIP biases^[19,20]. Other studies suggest differing composition between active regions despite roughly similar temperature distributions^[35]. In flares, some studies have shown a photospheric abundance for Fe but an enrichment for (lower-FIP) Ca^[36,37], while others show variations from flare to flare^[38,39]. An inverse FIP effect (Ar enhanced relative to Ca) has also been detected in sunspots^[40,41], and FIP bias and/or temperature distributions may even evolve over active region lifetimes^[42,43]. This variability suggests that the fractionation threshold may depend on details of the heating mechanism and properties of the ambient magnetic field. Systematic studies are clearly needed to make progress on this question, but abundance measurements from many flares and active regions over long periods of time have been very difficult to make with previous instrumentation.

Crucially, the existing studies used instruments with differing and restricted temperature and composition sensitivities, confounding efforts to reconcile conflicting results. For example, very few strong EUV lines are sensitive to the physically important 5–10 MK range^[44], and almost all available EUV lines at higher temperatures are from Fe, limiting abundance measurements of hot ions. Hard X-ray spectra above 10 keV have no prominent spectral lines and offer limited diagnostics of thermal plasma.

Spectrally resolved SXR observations, including both imaging and spatially-integrated spectroscopy, offer powerful diagnostics to reconcile these numerous issues. SXR emission is particularly sensitive to mid- and high-temperature plasma, ~2–50 MK, and includes strong emission lines from both low- and high-FIP elements (Fig. 2) across this temperature range, from O VIII (~2 MK) to Fe XXVI (\gtrsim 25 MK). The bright bremsstrahlung continuum in SXRs is sensitive to the same temperature range and, as it originates from free electrons, is also largely insensitive to potential ionization non-equilibrium conditions that can affect interpretation of line spectra; the continuum therefore provides strong independent temperature constraints for more accurate abundance determinations from line emission. SXR spectroscopic observations thus completely fill the

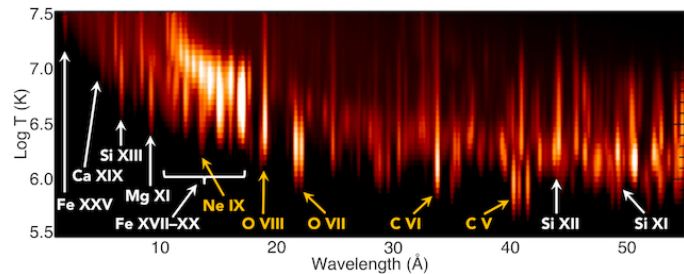


Fig. 2. SXR emission includes many spectral lines from hot ions, both low- (white text) and high-FIP (orange text), across the full range of coronal temperatures, from \sim 1 to $>$ 30 MK.

“blind spot” endemic to EUV measurements and provide unique insight into both quiescent and flaring coronal temperature distributions and composition^[44].

These same measurements hold promise to provide insights into closely-related questions in solar and space physics, including the mechanism of FIP fractionation, the origins of the solar wind (via comparison of SXR-derived and *in situ*-measured abundances) and its connections to coronal heating, and solar SXR forcing of dynamical processes in Earth’s ionosphere D and E regions.

In the near term, significant scientific progress can be made even with only modest spectral, spatial, and temporal resolution and signal-to-noise (SNR) available from existing low-cost and low-resource instrumentation. For example, current commercial off-the-shelf (COTS) silicon drift detectors (SDDs) and cadmium-telluride (CdTe) detectors provide high-sensitivity spectroscopy with broad passband and modest to good ($E/\Delta E \approx 10-100$) resolution even from CubeSat platforms^[45,46]. New rapid-readout pixelated CMOS imaging detectors^[47,48] enable similar spectroscopic performance with spatial resolution from ~ 10 arcsec using replicated focusing optics^[48] down to sub-arcsecond using emerging new developments. Rapid increases in computer processing power, even from low-cost hardware, have also enabled quantitative advances in imaging spectroscopy through “overlappograph” instruments where spectral and spatial information is overlaid on the same detector, e.g., slot or slitless spectrographs using diffraction gratings^[49-51]. Several such instruments have recently been proposed and offer the capability of fully spanning the 0.25–3 keV observational gap within the next few years.

Longer-term progress depends on maximizing sensitivity and spectral and spatial resolution across the widest possible passband. High-resolution ($E/\Delta E \gtrsim 1000$) spectroscopy enables detailed spectral diagnostics including for bulk velocities and turbulence from line broadening. Such resolution has long been available from crystal spectrometers using Bragg diffraction, but these instruments were typically complicated by very narrow passbands and contamination from fluorescence. Ongoing improvements in detector and materials technology hold promise to resolve these issues and enable high-performance spectroscopy over much broader passbands. Additional longer-term developments in superconducting transition-edge sensors and microcalorimeters offer the possibility of achieving crystal-like resolution with silicon-like sensitivity and passband, including in pixelated formats to enable super-high-resolution imaging spectroscopy.

Breakthrough progress in understanding coronal heating and other crucial scientific questions is possible via SXR spectroscopy, including imaging spectroscopy and spectropolarimetry. To achieve such progress within the next three decades, by 2050, it is imperative to invest in these emerging technologies and funding opportunities to enable rapid development and deployment of new SXR instruments and missions that can achieve groundbreaking new measurements.

References

- [1] Grotrian, W. 1939, *Naturwissenschaften*, **27**, 214
- [2] Edlén, B. 1943, *Zeitschrift für Astrophysik*, **22**, 30
- [3] Klimchuk, J.A. 2006, *Sol. Phys.*, **234**, 41
- [4] Welsch, B. T. 2014, *PASJ*, **67**, 18
- [5] Klimchuk, J. A., et al. 2020a, *Heliophysics 2050 Workshop*, white paper #4027
- [6] Klimchuk, J. A., et al. 2020b, *Heliophysics 2050 Workshop*, white paper #4028
- [7] Parker, E. N. 1988, *ApJ*, **330**, 474
- [8] Cargill, P. J., & Klimchuk, J. A. 2004, *ApJ*, **605**, 911
- [9] Cargill, P. J. 2014, *ApJ*, **784**, 49
- [10] van Ballegooijen, A. A., et al. 2011, *ApJ*, **736**, 3
- [11] Asgari-Targhi, M., et al. 2013, *ApJ*, **773**, 111
- [12] Miceli, M., et al. 2012, *A&A*, **544**, A139
- [13] Brosius, J. W., et al. 2014, *ApJ*, **790**, 112
- [14] Caspi, A., et al. 2015a, *ApJL*, **802**, L2
- [15] Sylwester, J., et al. 2012, *ApJ*, **751**, 111
- [16] Schrijver, C. J., et al. 1998, *Nature*, **394**, 152
- [17] Reale, F., et al. 2009, *ApJ*, **698**, 756
- [18] Schmelz, J. T., et al. 2009, *ApJL*, **693**, L131
- [19] Warren, H. P., et al. 2012, *ApJ*, **759**, 141
- [20] Del Zanna, G., & Mason, H. E. 2014, *A&A*, **565**, A14
- [21] Caspi, A., & Lin, R. P. 2010, *ApJ*, **725**, 161
- [22] Caspi, A., et al. 2014, *ApJ*, **781**, 43
- [23] Fletcher, L., et al. 2011, *Space Sci. Rev.*, **159**, 19
- [24] Holman, G. D., et al. 2011, *Space Sci. Rev.*, **159**, 107
- [25] Allred, J. C., et al. 2005, *ApJ*, **630**, 573
- [26] Allred, J. C., et al. 2015, *ApJ*, **809**, 104
- [27] Liu, W.-J., et al. 2013, *ApJ*, **770**, 111
- [28] Aschwanden, M. J., et al. 2015, *ApJ*, **802**, 53
- [29] Caspi, A., et al. 2015b, *ApJL*, **811**, L1
- [30] Aschwanden, M. J., et al. 2016, *ApJ*, **832**, 27
- [31] Warmuth, A., & Mann, G. 2016, *A&A*, **588**, A116
- [32] Longcope, D. W., & Guidoni, S. E. 2011, *ApJ*, **740**, 73
- [33] Shih, A. Y., et al. 2020, *Heliophysics 2050 Workshop*, white paper #4023
- [34] Laming, J. M. 2015, *Liv. Rev. Sol. Phys.*, **12**, 2
- [35] Wieman, S., et al. 2015, *AGU Fall Meeting*, #SH23B-2446
- [36] Warren, H. P. 2014, *ApJ*, **786**, L2
- [37] Dennis, B. R., et al. 2015, *ApJ*, **803**, 67
- [38] Sylwester, J., et al. 1984, *Nature*, **310**, 665
- [39] Schmelz, J. T. 1993, *ApJ*, **408**, 373
- [40] Doschek, G. A., et al. 2015, *ApJ*, **808**, 7
- [41] Doschek, G. A. & Warren, H. P. 2016, *ApJ*, **825**, 36
- [42] Widner, K. G., & Feldman, U. 2001, *ApJ*, **555**, 426
- [43] Baker, D., et al. 2015, *ApJ*, **802**, 104
- [44] Winebarger, A. R., et al. 2012, *ApJL*, **746**, L17
- [45] Mason, J. P., et al. 2016, *J. Spacecraft Rockets*, **53**, 328
- [46] Moore, C. S., et al. 2018, *Sol Phys.*, **293**, 21
- [47] Soman, M., et al. 2016, *Proc. SPIE*, **9915**, 991540
- [48] Narukage, N., et al. 2017, *Proc. SPIE*, **10397**, 1039709
- [49] Tousey, R., et al. 1977, *Appl. Optics*, **16**, 870
- [50] Golub, L., et al. 2020, *J. Space Weather Space Climate*, **10**, 37
- [51] Caspi, A., et al. 2016, *Proc. SPIE*, **9905**, 9905226